doi: 10.18323/2782-4039-2024-4-70-9

Effect of alloy composition on machining parameters and surface quality through comprehensive analysis

Shailesh Rao A.*[1], PhD, Professor, Department of Mechanical Engineering
Srilatha Rao[2], PhD, Professor
Nitte Meenakshi Institute of Technology, Bangalore (India)

***E-mail:** shailesh.rao@nmit.ac.in

[1]ORCID: https://orcid.org/0000-0001-6190-9857
[2]ORCID: https://orcid.org/0000-0003-3691-8713

Received 25.04.2024 *Revised 18.06.2024* *Accepted 05.11.2024*

Abstract: This study examined the influence of alloy composition (mild steel and aluminium) on several machining parameters, such as temperature, cutting force, surface roughness, and chip morphology. Significant variations in these parameters were detected by modifying the alloys while maintaining constant process conditions. In mild steel, rotating speed affected chip morphology, with elevated speeds resulting in continuous chips and reduced rates yielding shorter chips. The augmented rake angle affects the chip properties, resulting in a little decrease in chip length. Moreover, the cutting force influenced the chip length at a designated rotational speed. Conversely, aluminium alloys continuously generated continuous chip fragments irrespective of cutting speed or rake angle. Favourable correlation coefficients are noted among the variables, and a regression model is effectively developed and utilised on the experimental data. The random forest model, indicates that material selection significantly influences temperature, cutting force, surface roughness, and chip morphology during machining. This study offers significant insights into the correlation between tool rake angle and other machining parameters, elucidating the elements that influence surface quality. The results enhance comprehension of machined surface attributes, facilitating the optimisation of machining operations for various materials.

Keywords: turning process; rake angle; chip morphology; predictive modelling.

For citation: Shailesh Rao A., Rao S. Effect of alloy composition on machining parameters and surface quality through comprehensive analysis. *Frontier Materials & Technologies*, 2024, no. 4, pp. 97–110. DOI: 10.18323/2782-4039-2024-4-70-9.

INTRODUCTION

The cylinder components with specified models are made using lathes and/or CNC machines. During the process, the chip detaches from the workpiece because of shear forces applied by a sharp tool. Recent advancements in research activities during the machining process have led to improved output quality. Dogra elucidated the importance of tool geometry in the turning process. The substantial heat generated during chip removal from the workpiece results in tool fatigue and inferior surface finish [1]. The importance of tool geometry throughout the machining process must be accurately articulated. Duc Pham Minh examined the influence of rake angle on material and chip properties. The variation in rake angle with different process conditions resulted in variation in tool wear, surface roughness and distinct chip morphologies [2].

The ductile material produces a continuous chip and offers a longer tool life compared to brittle material, which generates a discontinuous chip and has a shorter tool life [3]. Numerous investigations demonstrated the correlation between a tool's morphology and its durability, as well as its surface irregularities. Tools with a larger radius operating at higher speeds resulted in lower surface roughness compared to those with a smaller radius. Analytical and numerical methods are currently utilised to obtain extensive information on the parameters of the cutting process [4]. Two-dimensional or three-dimensional models are employed in simulation methodologies to illustrate the diverse cutting parameters and materials [5]. Many models rely on a two-dimensional framework, and are not implemented in three dimensions due to heightened computational time and complexity [6].

The proliferation of diverse commercial products has escalated due to the swift technical advancements of the modern environment. Li Bin examined the advancements in theoretical analysis and numerical modelling of tool wear globally [7]. Outeiro conducted numerical modelling and simulation of metal cutting procedures. Numerous numerical methods, including Finite Element method (FEM) and Mesh-free techniques, are being developed to simulate machining operations [8]. The ABAQUS algorithm was employed to model the oblique cutting of nickel-based alloys using coated tools, resulting in a more accurate prediction of cutting forces [9]. The comparison of simulation findings with experimental data revealed that the simulation results aligned with the experimental outcomes. The FEM tool was employed to provide a thorough analysis of the effects of key machining variables on the mechanical properties of mild steel alloys machined using a ceramic tool. The simulation generated a distributed representation of temperature and stress values in the tool tip during the analysis [10]. The simulation or FEM-based approaches are utilised solely for calculating results; they cannot be compared with other process factors or subjected to comprehensive analysis. Various tools, including MATLAB, ANOVA, and open-source software such as R and Python, are utilised to compare and predict output variables with different predictors. Regression models are employed to ascertain the link between several independent factors, and a dependent variable for future predictions. Numerous numerical algorithms were created from the experimental data collected during the machining process. The selection of suitable predictive models facilitates the determination of optimal cutting parameters and enhances process quality [11; 12]. The researchers have developed predictive models to enhance tool longevity [13], minimise machining duration [14], decrease energy usage [15], and reduce setup time [16], among other factors. These models are crucial for determining optimal cutting parameters and enhancing procedural quality. Li Kuan-Ming and Liang Steven Y. devised a temperature model to forecast tool temperature during oblique rotation, thereby elucidating the stability of the machining process [17]. Ko Jeong Hoon devised a model for attrition rates during the milling process [18]. It is essential to thoroughly investigate the influence of rake angles on different materials to create dependable forecast models. Consequently, further research is necessary to develop predictive models that juxtapose steel with aluminium. The shape of the cutting tool is a critical machining parameter that affects cutting conditions, and consequently, the quality of the completed products[1]. A comprehensive understanding of how material properties influence the cutting technique, necessitates a meticulous examination of chip morphology across various materials under defined process parameters.

The primary aim of this study is to analyse machining parameters, including temperature, cutting force, surface roughness, and chip morphology, with the varying alloy compositions.

The objective of the work is to enhance comprehension of the effects of material selection and tool rake angle on surface quality, chip morphology, and other machining results, hence facilitating the optimisation of machining processes for diverse materials. To enhance the outcomes, predictive analysis must be conducted to comprehend surface morphology with varying material compositions.

METHODS

In the present work, the turning process are carried out with aluminium and steel alloys, with varying rake angle as one of the machining parameters. The other possible combination of process parameters, such as cutting velocity, cutting force, surface texture, and temperature are also carried out and quantified. The investigations were conducted utilising a PSG 124 / A 124 heavy-duty precision lathe machine produced by HMT Machine Tools Ltd. (Hindustan Machine Tools, India). Two specimens, mild steel (EN9) and aluminium (2017-T4), exhibiting comparable mechanical properties as per ASM handbooks, are selected as the workpiece materials. The workpieces measured 24 mm in diameter and 150 mm in length. The specimens were firmly secured in a three-jaw chuck and revolved at cutting speeds of 160 rpm and 360 rpm, maintaining a constant feed rate of 0.12 mm/rev. We employed an Indian-manufactured high-speed steel tool containing 10 % cobalt, featuring a square cross-section of 12.7 mm and a length of 50 mm. We adjusted the tool rake angles (3°, 5°, 8°, and 11°) and taken a depth of cut of 0.5 mm as process parameters. A typical lathe tool dynamometer was affixed to the lathe machine to measure the forces produced during machining. The profile projector was utilised to analyse chip formation and ascertain the length of the chip's serrations from enlarged images. The surface roughness was assessed using an SJ-218 Talysurf (Mitutoyo, Japan) on the machined surface.

With the detailed experiment values, a predictive model is proposed to provide an early assessment of the relationship between variables, focusing on temperature as the output. The R software tool is employed to create a predictive model utilising experimental data. The study was conducted by importing the data into the tool environment. The "read.csv()" function was employed to import the tabular data, with appropriate formatting and variable allocation. The correlation coefficients between the dependent and independent variables are computed first from the available data. Additionally, linear regression and the random forest technique are employed to forecast surface roughness based on provided data.

RESULTS

Chip formation

The chip formation provides insight into the workpiece quality and dictates machining stability. Fig. 1 illustrates the chip pictures on the profile projectors and facilitates the measurement of chip geometry. Initial observations indicate that alterations in the rake angle have affected the chip length. This phenomenon results from a change in the direction of chip flow across the blade's surface. Significantly, at 140 rpm, an increase in cutting force led to the formation of shorter chips. The properties of aluminium alloys led to the generation of continuous chips, irrespective of variations in cutting speed or rake angle, as illustrated in Fig. 1.

Determination of properties during the machining process

Fig. 2 a illustrates the serration height observed during the chip study at various cutting rates. The height rises as the spinning speed diminishes. At elevated rotating velocities, a continuous chip is produced with curls. Throughout the procedure, the tool tip engages with the work material, undergoes compression, and attains a plastic state. A longer serration length is noticed when mild steel is rotated at

[1] *Dogra M., Sharma V.S., Dureja J.S. Effect of tool geometry variation on finish turning – A Review. Journal of Engineering Science and Technology Review, 2011, vol. 4, no. 1, pp. 1–13. DOI: 10.25103/jestr.041.01.*

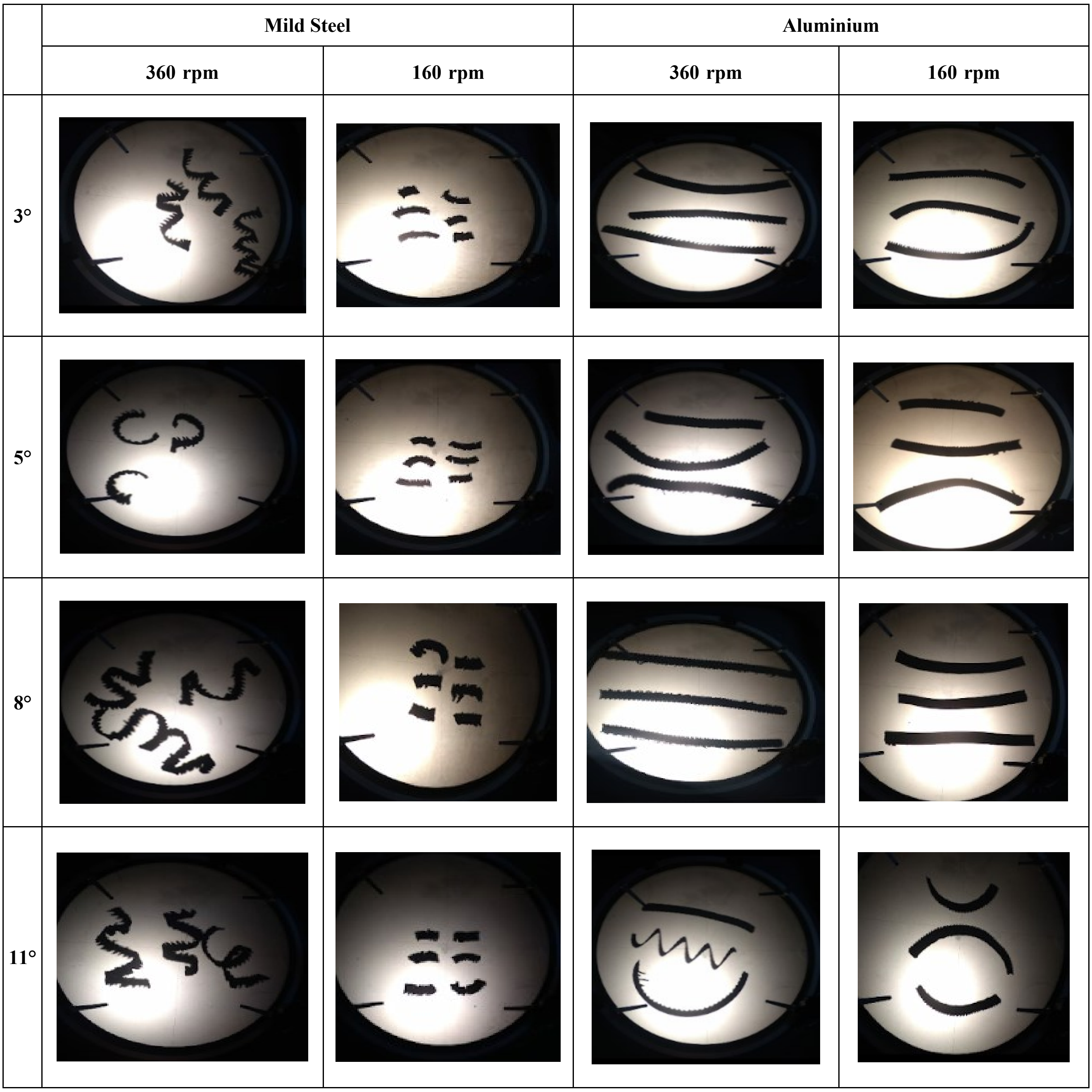

Fig. 1. *Chip formation for the different materials at different rake angles and rotational speeds*
Рис. 1. *Образование стружки для различных материалов при различных углах наклона и скоростях вращения*

a reduced speed. In aluminium alloys, a constant material removal thickness produces an elongated fragment with a reduced serration length.

Fig. 2 b illustrates the roughness values of the machined surface. For mild steel, these values diminished with an increase in cutting speed. The results indicate that its value is inversely related to the cutting temperature. Elevated cutting temperatures promote the thermal softness of the material, hence allowing for the facile extraction of the metal from the alloy. Moreover, an escalation in cutting speed amplifies surface-level vibrations and thermal generation. This leads to the creation of a coarse surface, which may also occur due to the disruption of the chip between the tool tip and the pliable workpiece. In the machining process, an increase in the rake angle results in a reduction of cutting force due to diminished contact at the tool tip interface. Fig. 3 a illustrates that the fragment length grows until a rake angle of 5°, after which it diminishes. The temperature at the tool tip contact is measured using a pyrometer and illustrated in Fig. 3 b. Here the temperature increases with a higher rake angle and the chosen material. This may arise from the higher frictional force.

Table 1 delineates the experimental data for various process parameters, including rotational speed, cutting force, rake angle, and surface roughness, along with their corresponding output variables.

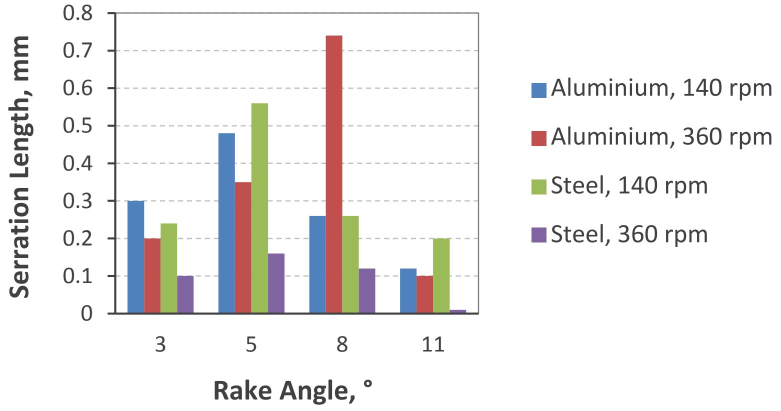

a

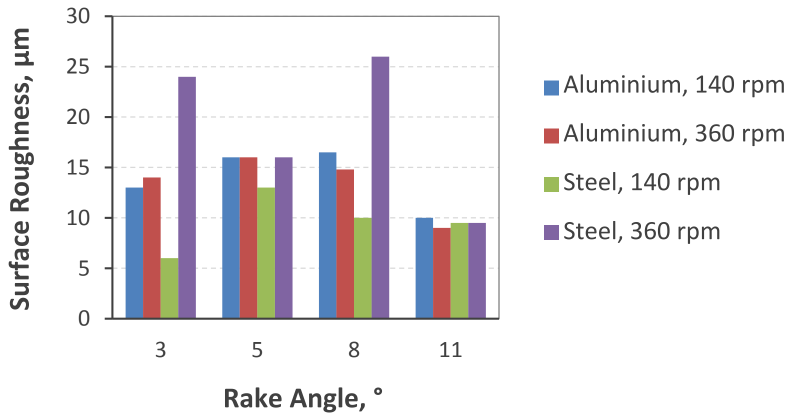

b

Fig. 2. *Determination of some mechanical properties during the machining process*
Рис. 2. *Определение некоторых механических свойств во время процесса обработки*

Table 2 shows the correlation values obtained from the analysis in the R software. The relationships between the different independent variables, and temperature are analysed using these coefficients. In this instance, surface roughness and cutting force have strong positive correlations with temperature. This acknowledges that an increase in surface roughness, and cutting force correlates with a rise in temperature throughout the machining process. These variables significantly influence the thermal behaviour of the process. The rake angle exhibits a moderate correlation with surface roughness. It exerts a minimal influence on the other variables in the study. The temperature had the most positive correlation with surface area and cutting force among the examined parameters. This indicates that the surface characteristics and cutting force produced during machining are directly correlated, with the resultant temperature. The correlation analysis revealed substantial correlations between these variables and the recorded temperature. Moreover, surface roughness and cutting force exhibited a negative correlation with the rake angle, as demonstrated in Table 2.

Multiple regression analysis showed that the cutting force, surface roughness, rake angle, and cutting speed significantly influenced the temperature generated at the contact during the studies. Tables 3 and 4 present the machining parameter values for aluminium and steel, respectively. For the provided data, the following response models are proposed for aluminium and steel:

Linear Regression for Steel

$$T = 199.64 - 0.05Fc - 0.1Ra + 6.482\gamma + 0.077SFM ,$$

where T is temperature;
Fc is cutting force;
Ra is surface roughness;
γ is rake angle;
SFM is cutting speed.

Linear Regression for Aluminium

$$T = 116.41 - 0.02Fc - 0.05Ra + 2.66\gamma + 0.132SFM .$$

To enhance performance in machining, it is essential to comprehend the correlation between process parameters and temperature. The experimental results underscore the temperature sensitivity of cutting force, cutting speed, surface roughness, and rake angle. In both equations, the p-values for independent variables with interaction factors were below 0.05, signifying that these variables exerted a statistically significant positive effect on temperature. The use of interaction terms indicates that

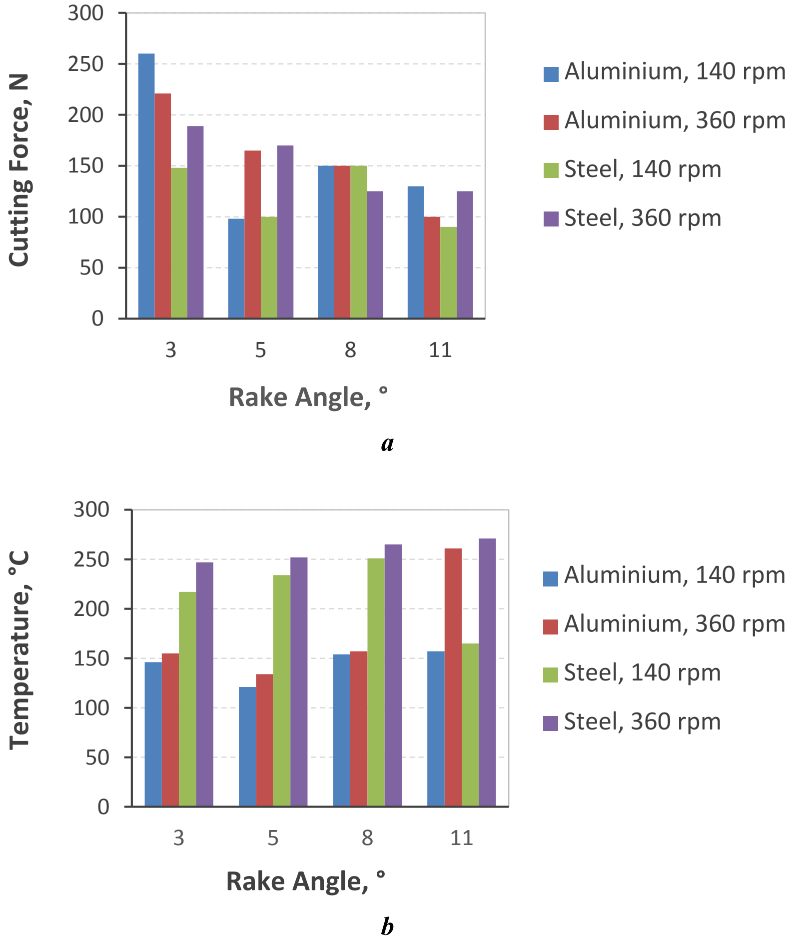

Fig. 3. *Temperature distribution for various rake angle*
Рис. 3. *Распределение температуры для различных передних углов*

the connection between temperature and the examined variables, is shaped by their interactions rather than being merely additive.

The *R*-squared values for both models were approximately 89 %, indicating their validity and goodness of fit. The elevated figures suggest that the models, grounded in the independent variables and their interactions, account for a substantial proportion of the temperature variance. The temperature regression analysis produced negligible residual values, signifying that the developed models effectively depict the relationship between the independent variables and temperature. The minimal residuals suggest that the models accurately approximate the actual temperature data.

Fig. 4 illustrates the actual and forecasted temperature measurements as depicted in R program. The graphical representation indicates that the temperature model was more precise than the stated process parameters. This confirms the efficacy of the developed models for forecasting temperature throughout the machining process.

The "plot3d" function from the "rgl" package is utilised to create a three-dimensional plot in R programming. The "plot3d" function is employed in this work to illustrate the correlation among force, cutting speed, and temperature for aluminium and steel alloys, as depicted in Fig. 5 a. From the figure, the cutting force diminishes with an increase in cutting speed across different rake angles. As the cutting speed increases, the temperature escalates. From the Fig. 5 b, an increase in the temperature is observed due to the alloy's hardness, which complicates its removal from the work surface. Furthermore, the tool tip conforms to the workpiece surface, elevating temperature. The effectiveness of the machining process is mostly influenced by the material of the workpiece and the configuration of the tool. Augmenting the rake angle improves the adhesion between the material surface and the rake surface of the instrument. This results in an increase in temperature, as illustrated in Fig. 6 a and 6 b. An increase in the hardness of the steel alloy resulted in a rise in temperature.

Fig. 7 illustrates the correlation between machined surface roughness, cutting speed, and temperature. As the rake angle is augmented, the surface irregularity initially escalates and subsequently diminishes. These observations were conducted for both alloys and two separate cutting rates. The machined surface value increased at a rake angle between 3° and 5°. The alteration in rake angle for aluminium elevated the roughness value from 14–15 µm to 17–18 µm at both cutting rates. This is mostly due to the establishment of lower temperatures at the tool tip contact. An increased rake angle results in the temperature shifting towards the centre of the workpiece,

Table 1. *Tabulated values of process parameters for steel and aluminium*
Таблица 1. *Табличные значения параметров процесса для стали и алюминия*

Material	Surface Roughness, µm	Cutting Force, N	Rake Angle, °	Temperature, °C	Speed, rpm	Peak Height, mm
Aluminium	13	260	3	136	140	0.3
	14	220	3	167	360	0.205
	17	100	5	141	140	0.48
	17	160	5	169	360	0.37
	17.5	150	8	143	140	0.27
	14.5	150	8	174	360	0.75
	10	125	11	151	140	0.13
	6.5	95	11	178	360	0.10
Steel	7	125	3	221	140	0.24
	24	190	3	243	360	0.12
	13	110	5	234	140	0.58
	17	170	5	253	360	0.17
	11	150	8	252	140	0.20
	27	120	8	257	360	0.13
	7	85	11	263	140	0.185
	7	125	11	289	360	0.015

Table 2. *Correlation values for steel and aluminium under different process parameters*
Таблица 2. *Значения корреляции для стали и алюминия при различных параметрах процесса*

	Steel			Aluminium		
	Roughness	Cutting Force	Rake Angle	Roughness	Cutting Force	Roughness
Roughness	1	–	–	1	–	–
Cutting Force	0.49	1	–	0.19	1	–
Rake Angle	−0.34	−0.57	1	−0.58	−0.72	1
Temperature	0.63	0.52	0.42	0.42	0.60	0.52
Cutting Speed	0.627	0.53	–	0.19	0.48	–

due to its elevated thermal conductivity. Throughout the machining process, the machined surface grows smoother, even with a slight increase in temperature. This diminishes surface roughness as fragments are readily removed from the workpiece. The roughness value diminished as the rake angle climbed to 8° and 11° owing to heat dissipation, through conduction and material softening.

For steel, a tougher material requires an increased cutting force to detach particles from the workpiece. Surface roughness escalates with an increase in rake angle, yet diminishes as built-up edge (BUE) or built-up layer (BUL)

Table 3. *The process parameter values during the machining of aluminum and its corresponding values*
Таблица 3. *Параметры процесса при обработке алюминия и соответствующие им значения*

Roughness, µm	Cutting Force, N	Rake Angle, °	Cutting Speed, rpm	Temperature		Residuals
				Actual	Regression Value	
13	260	3	140	135	137.735	−0.02026
14	220	3	360	168	167.580	0.00250
17	100	5	140	146	146.275	−0.00188
17	160	5	360	172	174.115	−0.01230
17.5	150	8	140	152	153.2575	−0.00827
14.5	150	8	360	182	182.2825	−0.00155
10	125	11	140	162	161.700	0.001852
6.5	95	11	360	190	191.3225	−0.00696

Table 4. *The process parameter values during the machining of steel and their corresponding values*
Таблица 4. *Параметры процесса при обработке стали и соответствующие им значения*

Roughness, µm	Cutting Force, N	Rake Angle, °	Cutting Speed, rpm	Temperature		Residuals
				Actual	Regression Value	
7	125	3	140	220	222.916	−0.013250
24	190	3	360	238	234.906	0.013000
13	110	5	140	235	236.030	−0.004380
17	170	5	360	254	249.570	0.017441
11	150	8	140	255	253.676	0.005192
27	120	8	360	268	270.516	−0.009390
7	85	11	140	270	276.772	−0.025080
7	125	11	360	290	291.712	−0.005900

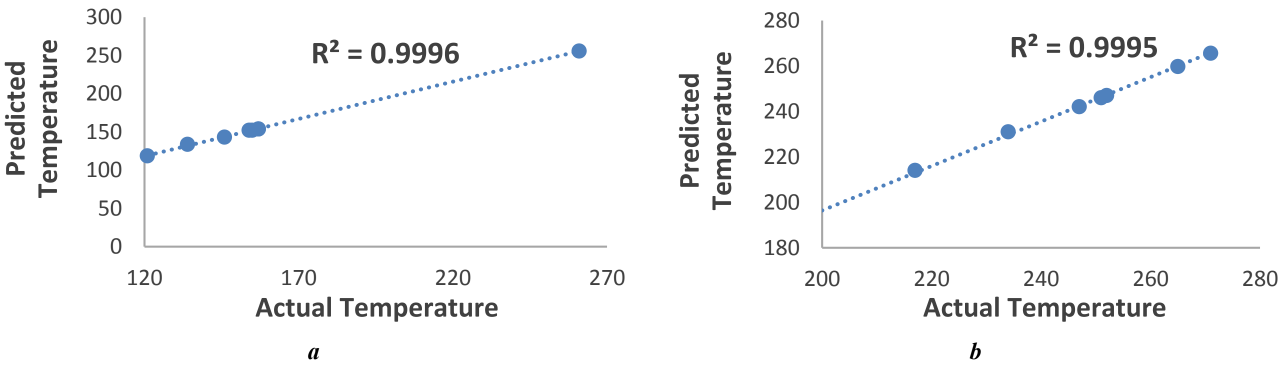

Fig. 4. *Comparison of actual temperature and predicted temperature value for aluminium (**a**) and steel (**b**)*
Рис. 4. *Сравнение фактического и прогнозируемого значений температуры для алюминия (**a**) и стали (**b**)*

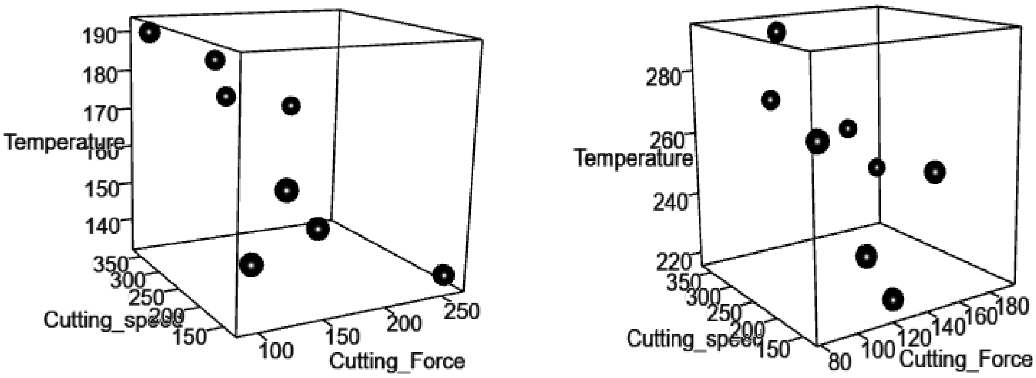

a *b*

Fig. 5. *Variation of cutting force and cutting speed with temperature for aluminium (**a**) and steel (**b**)*
Рис. 5. *Изменение силы и скорости резания в зависимости от температуры для алюминия (**a**) и стали (**b**)*

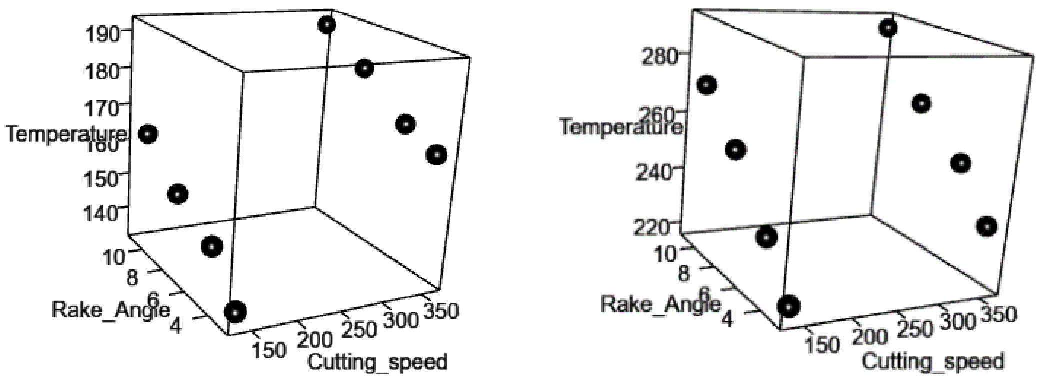

a *b*

Fig. 6. *Variation of rake angle and cutting speed with temperature for aluminium (**a**) and steel (**b**)*
Рис. 6. *Изменение переднего угла и скорости резания в зависимости от температуры для алюминия (**a**) и стали (**b**)*

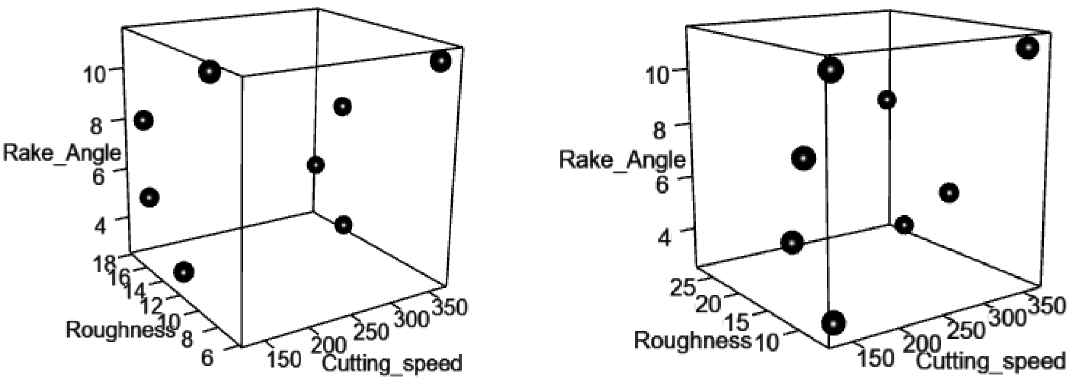

a *b*

Fig. 7. *Variation of roughness and cutting speed with rake angle for aluminium (**a**) and steel (**b**)*
Рис. 7. *Изменение шероховатости и скорости резания в зависимости от переднего угла для алюминия (**a**) и стали (**b**)*

develops at the tool tip contact and the material undergoes softening. In comparison to aluminium, steel exhibits lower heat conductivity, and Fig. 8 a illustrates an elevation in cutting temperature. Surface roughness escalates with an increase in rake angle and cutting speed.

Random Forest is considered one of the most efficient categorisation approaches in machine learning. This methodology is used for a dataset comprising several process parameters of two distinct alloys. Notwithstanding the dataset's very limited size, the Random Forest algorithm effectively identified alterations in alloy properties depending on their processing features. From the dataset shown in Table 1, 70 % of the data points were allocated for the training set to facilitate precise model evaluation, while the remaining 30% were designated for validation. The models' consistency was assessed using Fig. 8 a, which illustrated their performance throughout an increased number of decision trees. The graph indicated a positive correlation between the quantity of trees and model stability, suggesting that an increase in the number of trees enhanced the reliability of the classification results. All numerical results must be displayed in the section bearing the same title. Moreover, Fig. 8 b demonstrated the variables' reliance on material selections. Significantly, in comparison to steel and aluminium, the peak length exhibited a substantial association (about 55 % of the total) among the alloys. The maximum height was mostly influenced by the material's strength and composition throughout the turning process. Moreover, these material characterristics accounted for roughly 35 % of the temperature fluctuation during machining.

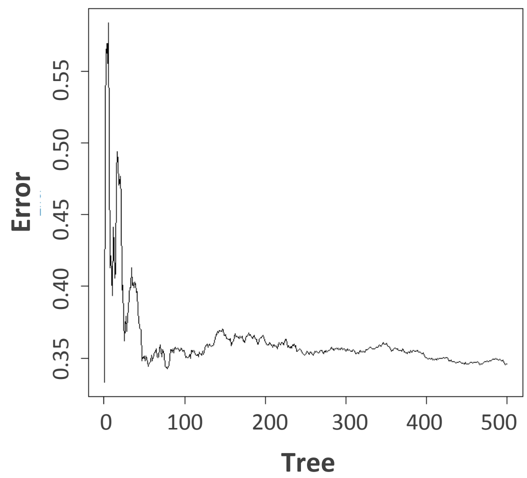

a

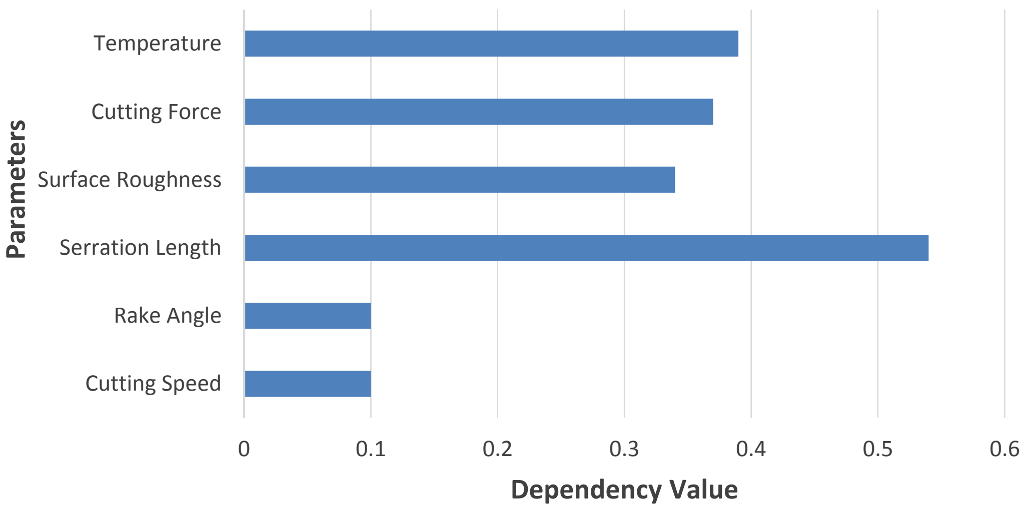

b

Fig. 8. *Error plot during the Random Forest model iteration* ***(a)***
and dependency plot between the variables for the material selection as output ***(b)***
Рис. 8. *Значимость параметров модели, полученная для случайного леса, по степени влияния на выходной параметр* ***(a)***
и график зависимости между переменными для выбора материала в качестве выходных данных ***(b)***

DISCUSSION

The chip formation provides insight into the workpiece quality and dictates machining stability. Continuous chips are generated when ductile materials are machined. This is mostly attributable to plastic deformation inside the work material. Inadequate cutting settings will lead to the generation of discontinuous chips when milling ductile and brittle materials. Substantial chip burrs are generated during milling under situations of elevated friction. This results from the frictional resistance and the formation of built-up edges at the tool tip's location. This study found that higher rotational speeds produced continuous chips in mild steel, while lower speeds yielded shorter chips [19]. This phenomenon can be elucidated by the inverse correlation between cutting speed and compressive stress, whereby an increase in cutting speed lowers compressive stress, facilitating the formation of continuous chips. Moreover, an increase in the rake angle resulted in a heightened serration elevation. This phenomenon is attributed to heightened segmentation and challenges in shear sliding, resulting in greater material being split off at each peak.

The alteration in rake angle also affected chip length, leading to a slight decrease in mild steel chips. This phenomena results from a change in the direction of chip flow across the blade's surface. Significantly, at 140 rpm, an augmentation in cutting force led to the formation of shorter chips. The properties of aluminium alloys led to the generation of continuous chips, irrespective of variations in cutting speed or rake angle. The morphological features of the fragments remained mostly unaltered despite modifications to these parameters.

The serration height was analysed in relation to varying cutting rates. The height rises as the spinning speed diminishes. At elevated rotating velocities, a continuous chip is produced with curls. Throughout the procedure, the tool tip encounters the work material, undergoes compression, and attains a plastic state. A longer serration length is noticed when mild steel is rotated at a reduced speed. This is mostly attributable to the increased stress that has arisen on the work surface. During machining, the material exhibits characteristics akin to those of a brittle substance. Augmenting the rake angle elevates the compressive stress [20]. In aluminium alloys, a constant material removal thickness yields an elongated fragment with a reduced serration length.

The surface roughness values of the machined area. For mild steel, these values diminished with an increase in cutting speed. The results indicate that its value is inversely related to the cutting temperature. Elevated cutting temperatures promote the thermal softness of the material, hence allowing for the facile extraction of the metal from the alloy [21]. The alloy's thermal softening at elevated temperatures is attributed to the ideal values of frictional energy, and shear plane energy [22]. The potential for elevated temperatures at the tool tip, facilitates the softening of the machined surface area. Demirpolat [23] and Martins [24] elucidate that an elevation in cutting speed diminishes the surface roughness of aluminium alloys, leading to reduced serration lengths. Moreover, an escalation in cutting speed amplifies surface-level vibrations and thermal generation. This leads to the creation of a rough surface, potentially caused by the disruption of the chip between the tool tip and the pliable workpiece. Augmenting the tiny rake angle diminishes the contact point, hence progressively reducing the cutting force [25]. The generation of vibrations may lead to the development of a surface with an irregular texture. Increasing the rake angle to 11° enhances the surface finish [26].

In the machining process, an increase in rake angle results in a reduction of cutting force due to diminished contact at the tool tip interface [27; 28]. Fig. 3 a illustrates that the fragment length grows until a rake angle of 5°, after which it diminishes. The temperature at the tool tip contact is measured using a pyrometer and depicted in Fig. 3 b. Here the temperature increases with a larger rake angle and the chosen material. This may result from the heightened frictional force.

From the Table 2, the surface roughness and cutting force have strong positive correlations with temperature. This acknowledges that an increase in surface roughness and cutting force correlates with a rise in temperature throughout the machining process. These variables significantly influence the thermal behaviour of the process. The rake angle exhibits a moderate correlation with surface roughness. It exerts a minimal influence on the other variables in the study. The temperature had the most positive correlation with surface area and cutting force among the examined parameters. This indicates that the surface characteristics and cutting force produced during machining are directly correlated with the resultant temperature. The correlation analysis revealed substantial correlations between these variables and the recorded temperature. Additionally, surface roughness and cutting force exhibited a negative correlation with the rake angle.

Further, the cutting force diminishes as the cutting speed escalates over different rake angles as referred from Fig. 5 a. Here the reduction in cutting force is due to the diminished chip-tool interaction. As the cutting speed escalates, the temperature increases. As a result, the yield strength diminishes with the rise in cutting speed [29]. The strong thermal conductivity and low hardness of aluminium alloys, during machining enabled the efficient removal of material from the workpiece. In contrast to steel alloys, a considerable quantity of heat is dissipated across the chip area, leading to a reduction in temperature. BUE is generated at an increased cutting speed with steel. As observed from Fig. 5 b, at a lower cutting velocity, a rise in temperature is seen due to the alloy's hardness, which complicates its removal from the work surface. Furthermore, the tool tip conforms to the workpiece surface, elevating temperature. The effectiveness of the machining process is mostly influenced by the material of the workpiece, and the configuration of the tool.

Overall, the rake angle substantially influences the temperature produced at the tool's interface. The augmentation of thrust force resulted in a temperature elevation of both materials. The alteration of the rake profile leads to the development of the BUE and BUL beneath the chip surface in contact with the rake surface. This results in an increase in temperature, as illustrated in Figs. 6 a and 6 b.

With the increase in the cutting speed, the cutting temperature reduces and similar observations are made from [30], where it was observed that the BUE and BUL diminishes with an increase in cutting speed (depth of cut is 0.15 mm).

Fig. 7 illustrates the correlation between machined surface roughness, cutting speed, and temperature. Here the machined surface value increased at a rake angle of 3° to 5°. This is mostly due to the establishment of lower temperatures at the tool tip contact. An increased rake angle results in the temperature shifting towards the centre of the workpiece due to its elevated thermal conductivity. Throughout the machining process, the machined surface grows smoother, even with a slight increase in temperature. This diminishes surface roughness as fragments are readily removed from the workpiece. The roughness value diminished as the rake angle climbed to 8° and 11° owing to heat loss through conduction, and the softening of the materials. For steel, a tougher material requires an increased cutting force to detach particles from the workpiece. The surface roughness escalates with an increase in rake angle, although diminishes as BUE or BUL develops at the tool tip interface and the material undergoes softening. In comparison to aluminium, steel exhibits lower thermal conductivity, here a reduction in surface roughness is noticed finally.

CONCLUSIONS

The tool rake angle is one of the most important factors to access the machining parameters during a turning process. A variation in temperature at the tool tip contact can be attributed to the change in the rake angle, which also causes the surface roughness to change. In the current work, aluminium and steel alloys with comparable qualities are machined using the parameters that have been established for the procedure. The following are the findings and inferences that can be made from the work.

1. During the machining of mild steel specimen, a larger chip length is noticed with larger rotational speed. A smaller chip length is observed when the rotational speed is lower due to the reduction in the compressive stress, that occurs during machining. When working with soft aluminium alloys, continual lengthy chips are seen despite the difference in rotating speed.

2. The surface roughness of both alloys is increased with the increase in the cutting speed. The additional friction that has developed at the tool tip interface resulted in increased roughness.

3. The values of correlation observed between the variables have been determined to be satisfactory. In addition, the regression model has been constructed and has been successfully applied to the data from the trial.

4. The cutting force, cutting speed, rake angle, and surface roughness all have a significant impact on the temperature, that is generated at the interface between the tool and the workpiece.

5. The random forest model is started to comprehend the reliance on variables for the content that has been picked. During the machining process, it is understood that the material selection has a significant impact on the temperature, cutting force, surface roughness, and chip shape that are produced.

REFERENCES

1. Anand A., Behera A.K., Das S.R. An overview on economic machining of hardened steels by hard turning and its process variables. *Manufacturing Review*, 2019, vol. 6, pp. 1–9. DOI: 10.1051/mfreview/2019002.
2. Duc Pham Minh, Giang Le Hieu, Dai Mai Duc, Sy Do Tien. An experimental study on the effect of tool geometry on tool wear and surface roughness in hard turning. *Advances in Mechanical Engineering*, 2020, vol. 12, no. 9, pp. 1–11. DOI: 10.1177/1687814020959885.
3. Rao A.S. Effect of nose radius on the chip morphology, cutting force and tool wear during dry turning of Inconel 718. *Tribology – Materials Surfaces & Interfaces*, 2023, vol. 17, no. 1, pp. 62–71. DOI: 10.1080/17515831.2022.2160161.
4. Bellini C., Di Cocco V., Iacoviello F., Sorrentino L. Numerical model development to predict the process-induced residual stresses in fibre metal laminates. *Forces in Mechanics*, 2021, vol. 3, article number 100017. DOI: 10.1016/j.finmec.2021.100017.
5. Mathivanan A., Swaminathan G., Sivaprakasam P., Suthan R., Jayaseelan V., Nagaraj M. DEFORM 3D Simulations and Taguchi Analysis in Dry Turning of 35CND16 Steel. *Advances in Materials Science and Engineering*, 2022, vol. 2022, no. 1, pp. 1–10. DOI: 10.1155/2022/7765343.
6. Mathivanan A., Sudeshkumar M., Ramadoss R., Ezilarasan C., Raju G., Jayaseelan V. Finite element simulation and regression modelling of machining attributes on turning AISI 304 stainless steel. *Manufacturing Review*, 2021, vol. 8, article number 24. DOI: 10.1051/mfreview/2021022.
7. Li Bin. A review of tool wear estimation using theoretical analysis and numerical simulation technologies. *International Journal of Refractory Metals and Hard Materials*, 2012, vol. 35, pp. 143–151. DOI: 10.1016/j.ijrmhm.2012.05.006.
8. Outeiro J.K., Umbrello D., M'Saoubi R., Jawahir I.S. Evaluation of Present Numerical models for Predicting Metal Cutting Performance and Residual Stresses. *Machining Science and Technology*, 2015, vol. 19, no. 2, pp. 183–216. DOI: 10.1080/10910344.2015.1018537.
9. Zheng Jin, Zhang Yaoman, Qiao Hanying. Milling Mechanism and Chattering Stability of Nickel-Based Superalloy Inconel 718. *Materials*, 2023, vol. 16, article number 5748. DOI: 10.3390/ma16175748.
10. Xiang Huimin, Xing Yan, Dai Fu-zhi et al. High-entropy ceramics: Present status, challenges, and a look forward. *Journal of Advanced Ceramics*, 2021, vol. 10, no. 3, pp. 385–441. DOI: 10.1007/s40145-021-0477-y.
11. Zhou Guo, Xu Chao, Wang Xiaohao, Feng Pingfa, Zhang Min. Determination of tool tip steady-state temperature in dry turning process based on artificial neural network. *Journal of Manufacturing Processes*, 2022, vol. 79, pp. 600–613. DOI: 10.1016/j.jmapro.2022.05.021.
12. Shailesh R.A. Surface finish and cutting efficiency in gingelly oil during machining: regression analysis.

Frontier Materials & Technologies, 2024, no. 2, pp. 101–111. DOI: 10.18323/2782-4039-2024-2-68-9.
13. Li Guo, Lu Wanqiu, Huang Shuchun, Zhang Xingyu, Ding Shuiting. Analysis and prediction of residual stresses based on cutting temperature and cutting force in rough turning of Ti–6Al–4V. *Heliyon*, 2022, vol. 8, no. 11, article number e11661. DOI: 10.1016/j.heliyon.2022.e11661.
14. Hegab H., Salem A., Rahnamayan S., Kishawy H.A. Analysis, modelling, and multi-objective optimisation of machining Inconel 718 with nano-additives based minimum quantity coolant. *Applied Soft Computing*, 2021, vol. 108, article number 107416. DOI: 10.1016/j.asoc.2021.107416.
15. Mhlanga D. Artificial Intelligence and Machine Learning for Energy Consumption and Production in Emerging Markets: A Review. *Energies*, 2023, vol. 16, no. 2, article number 745. DOI: 10.3390/en16020745.
16. Cai Wei, Li Yanqi, Li Li, Lai Kee-hung, Jia Shun, Xie Jun, Zhang Yuanhui, Hu Luoke. Energy saving and high efficiency production oriented forward-and-reverse multidirectional turning: Energy modelling and application. *Energy*, 2022, vol. 252, article number 123981. DOI: 10.1016/j.energy.2022.123981.
17. Li Kuan-Ming, Liang Steven Y. Modelling of cutting forces in near dry machining under tool wear effect. *International Journal of Machine Tools and Manufacture*, 2007, vol. 47, no. 7-8, pp. 1292–1301. DOI: 10.1016/j.ijmachtools.2006.08.017.
18. Ko Jeong Hoon. Time-domain prediction of milling stability according to cross edge radius and flank edge profiles. *International Journal of Machine Tools and Manufacture*, 2015, vol. 89, pp. 74–85. DOI: 10.1016/j.ijmachtools.2014.11.004.
19. Trujillo Vilches F.J., Hurtado L.S., Fernández F.M., Gamboa C.B. Analysis of the Chip Geometry in Dry Machining of Aeronautical Aluminium Alloys. *Applied Sciences*, 2017, vol. 7, no. 2, article number 132. DOI: 10.3390/app7020132.
20. Machado A.R., Da Silva L.R.R., De Souza F.C.R., Davis R., Pereira L.C., Sales W.F., De Rossi W., Ezugwu E.O. State of the art of tool texturing in machining. *Journal of Materials Processing Technology*, 2021, vol. 293, article number 117096. DOI: 10.1016/j.jmatprotec.2021.117096.
21. Radhika A., Shailesh Rao A., Yogesh K.B. Evaluating machining performance of AlSI 1014 steel using gingelly oil as cutting fluid. *Australian Journal of Mechanical Engineering*, 2021, vol. 19, no. 4, pp. 445–456. DOI: 10.1080/14484846.2019.1636517.
22. Agari S.R. Wear and surface characteristics on tool performance with CVD coating of Al_2O_3/TiCN inserts during machining of Inconel 718 alloys. *Archive of Mechanical Engineering*, 2021, vol. 69, no. 1, pp. 59–75. DOI: 10.24425/ame.2021.139647.
23. Demirpolat H., Binali R., Patange A.D., Pardeshi S.S., Gnanasekaran S. Comparison of Tool Wear, Surface Roughness, Cutting Forces, Tool Tip Temperature, and Chip Shape during Sustainable Turning of Bearing Steel. *Materials*, 2023, vol. 16, no. 12, article number 4408. DOI: 10.3390/ma16124408.
24. Martins P.S., Carneiro J.R.G., Ba E.C.T., Vieira V.F. Study on roughness and form errors linked with tool wear in the drilling process of an Al–Si alloy under high cutting speed using coated diamond-like carbon high-speed steel drill bits. *Journal of Manufacturing Processes*, 2021, vol. 62, pp. 711–719. DOI: 10.1016/j.jmapro.2021.01.006.
25. Zhuang Gullin, Liu Hanzhong, Zong Wenjun. Research on the Method of Reducing Dynamic Cutting Force in Aspheric Machining. *Micromachines*, 2023, vol. 14, no. 5, article number 960. DOI: 10.3390/mi14050960.
26. Ellersiek L., Menze C., Sauer F., Denkena B., Möhring H.-Ch., Schulze V. Evaluation of methods for measuring tool-chip contact length in wet machining using different approaches (microtextured tool, in-situ visualisation and restricted contact tool). *Production Engineering*, 2022, vol. 16, no. 5, pp. 635–646. DOI: 10.1007/s11740-022-01127-w.
27. Vukelic D., Simunovic K., Ivanov V., Sokac M., Kocovic V., Santosi V., Santosi Z., Simunovic G. Modelling of Flank and Crater Wear during Dry Turning of AISI 316L Stainless Steel as a Function of Tool Geometry Using the Response Surface Design. *Tehnicki Vjesnik – Technical Gazette*, 2024, vol. 31, no. 4, pp. 1376–1384. DOI: 10.17559/tv-20231226001235.
28. Younas M., Khan M., Jaffery S.H.I., Khan Z., Khan N. Investigation of tool wear and energy consumption in machining Ti6Al4V alloy with uncoated tools. *The International Journal of Advanced Manufacturing Technology*, 2024, vol. 132, no. 7-8, pp. 3785–3799. DOI: 10.1007/s00170-024-13548-1.
29. Çiftçi I. Machining of austenitic stainless steels using CVD multi-layer coated cemented carbide tools. *Tribology International*, 2006, vol. 39, no. 6, pp. 565–569. DOI: 10.1016/j.triboint.2005.05.005.
30. Gokkaya H., Taşkesen A. The effects of cutting speed and feed rate on BUE-BUL formation, cutting forces and surface roughness when machining AA6351 (T6) alloy. *Journal of Mechanical Engineering*, 2008, vol. 54, no. 7-8, pp. 521–530.

СПИСОК ЛИТЕРАТУРЫ

1. Anand A., Behera A.K., Das S.R. An overview on economic machining of hardened steels by hard turning and its process variables // Manufacturing Review. 2019. Vol. 6. P. 1–9. DOI: 10.1051/mfreview/2019002.
2. Duc Pham Minh, Giang Le Hieu, Dai Mai Duc, Sy Do Tien. An experimental study on the effect of tool geometry on tool wear and surface roughness in hard turning // Advances in Mechanical Engineering. 2020. Vol. 12. № 9. P. 1–11. DOI: 10.1177/1687814020959885.
3. Rao A.S. Effect of nose radius on the chip morphology, cutting force and tool wear during dry turning of Inconel 718 // Tribology – Materials Surfaces & Interfaces. 2023. Vol. 17. № 1. P. 62–71. DOI: 10.1080/17515831.2022.2160161.
4. Bellini C., Di Cocco V., Iacoviello F., Sorrentino L. Numerical model development to predict the process-induced residual stresses in fibre metal laminates // Forces in Mechanics. 2021. Vol. 3. Article number 100017. DOI: 10.1016/j.finmec.2021.100017.
5. Mathivanan A., Swaminathan G., Sivaprakasam P., Suthan R., Jayaseelan V., Nagaraj M. DEFORM 3D

Simulations and Taguchi Analysis in Dry Turning of 35CND16 Steel // Advances in Materials Science and Engineering. 2022. Vol. 2022. № 1. P. 1–10. DOI: 10.1155/2022/7765343.

6. Mathivanan A., Sudeshkumar M., Ramadoss R., Ezilarasan C., Raju G., Jayaseelan V. Finite element simulation and regression modeling of machining attributes on turning AISI 304 stainless steel // Manufacturing Review. 2021. Vol. 8. Article number 24. DOI: 10.1051/mfreview/2021022.
7. Li Bin. A review of tool wear estimation using theoretical analysis and numerical simulation technologies // International Journal of Refractory Metals and Hard Materials. 2012. Vol. 35. P. 143–151. DOI: 10.1016/j.ijrmhm.2012.05.006.
8. Outeiro J.K., Umbrello D., M'Saoubi R., Jawahir I.S. Evaluation of Present Numerical models for Predicting Metal Cutting Performance and Residual Stresses // Machining Science and Technology. 2015. Vol. 19. № 2. P. 183–216. DOI: 10.1080/10910344.2015.1018537.
9. Zheng Jin, Zhang Yaoman, Qiao Hanying. Milling Mechanism and Chattering Stability of Nickel-Based Superalloy Inconel 718 // Materials. 2023. Vol. 16. Article number 5748. DOI: 10.3390/ma16175748.
10. Xiang Huimin, Xing Yan, Dai Fu-zhi et al. High-entropy ceramics: Present status, challenges, and a look forward // Journal of Advanced Ceramics. 2021. Vol. 10. № 3. P. 385–441. DOI: 10.1007/s40145-021-0477-y.
11. Zhou Guo, Xu Chao, Wang Xiaohao, Feng Pingfa, Zhang Min. Determination of tool tip steady-state temperature in dry turning process based on artificial neural network // Journal of Manufacturing Processes. 2022. Vol. 79. P. 600–613. DOI: 10.1016/j.jmapro.2022.05.021.
12. Шайлеш Р.А. Качество обработки поверхности и эффективность резания в кунжутном масле во время механической обработки: регрессионный анализ // Frontier Materials & Technologies. 2024. № 2. С. 101–111. DOI: 10.18323/2782-4039-2024-2-68-9.
13. Li Guo, Lu Wanqiu, Huang Shuchun, Zhang Xingyu, Ding Shuiting. Analysis and prediction of residual stresses based on cutting temperature and cutting force in rough turning of Ti–6Al–4V // Heliyon. 2022. Vol. 8. № 11. Article number e11661. DOI: 10.1016/j.heliyon.2022.e11661.
14. Hegab H., Salem A., Rahnamayan S., Kishawy H.A. Analysis, modeling, and multi-objective optimization of machining Inconel 718 with nano-additives based minimum quantity coolant // Applied Soft Computing. 2021. Vol. 108. Article number 107416. DOI: 10.1016/j.asoc.2021.107416.
15. Mhlanga D. Artificial Intelligence and Machine Learning for Energy Consumption and Production in Emerging Markets: A Review // Energies. 2023. Vol. 16. № 2. Article number 745. DOI: 10.3390/en16020745.
16. Cai Wei, Li Yanqi, Li Li, Lai Kee-hung, Jia Shun, Xie Jun, Zhang Yuanhui, Hu Luoke. Energy saving and high efficiency production oriented forward-and-reverse multidirectional turning: Energy modeling and application // Energy. 2022. Vol. 252. Article number 123981. DOI: 10.1016/j.energy.2022.123981.
17. Li Kuan-Ming, Liang Steven Y. Modelling of cutting forces in near dry machining under tool wear effect // International Journal of Machine Tools and Manufacture. 2007. Vol. 47. № 7-8. P. 1292–1301. DOI: 10.1016/j.ijmachtools.2006.08.017.
18. Ko Jeong Hoon. Time-domain prediction of milling stability according to cross edge radius and flank edge profiles // International Journal of Machine Tools and Manufacture. 2015. Vol. 89. P. 74–85. DOI: 10.1016/j.ijmachtools.2014.11.004.
19. Trujillo Vilches F.J., Hurtado L.S., Fernández F.M., Gamboa C.B. Analysis of the Chip Geometry in Dry Machining of Aeronautical Aluminum Alloys // Applied Sciences. 2017. Vol. 7. № 2. Article number 132. DOI: 10.3390/app7020132.
20. Machado A.R., Da Silva L.R.R., De Souza F.C.R., Davis R., Pereira L.C., Sales W.F., De Rossi W., Ezugwu E.O. State of the art of tool texturing in machining // Journal of Materials Processing Technology. 2021. Vol. 293. Article number 117096. DOI: 10.1016/j.jmatprotec.2021.117096.
21. Radhika A., Shailesh Rao A., Yogesh K.B. Evaluating machining performance of AISI 1014 steel using gingelly oil as cutting fluid // Australian Journal of Mechanical Engineering. 2021. Vol. 19. № 4. P. 445–456. DOI: 10.1080/14484846.2019.1636517.
22. Agari S.R. Wear and surface characteristics on tool performance with CVD coating of Al_2O_3/TiCN inserts during machining of Inconel 718 alloys // Archive of Mechanical Engineering. 2021. Vol. 69. № 1. P. 59–75. DOI: 10.24425/ame.2021.139647.
23. Demirpolat H., Binali R., Patange A.D., Pardeshi S.S., Gnanasekaran S. Comparison of Tool Wear, Surface Roughness, Cutting Forces, Tool Tip Temperature, and Chip Shape during Sustainable Turning of Bearing Steel // Materials. 2023. Vol. 16. № 12. Article number 4408. DOI: 10.3390/ma16124408.
24. Martins P.S., Carneiro J.R.G., Ba E.C.T., Vieira V.F. Study on roughness and form errors linked with tool wear in the drilling process of an Al–Si alloy under high cutting speed using coated diamond-like carbon high-speed steel drill bits // Journal of Manufacturing Processes. 2021. Vol. 62. P. 711–719. DOI: 10.1016/j.jmapro.2021.01.006.
25. Zhuang Gullin, Liu Hanzhong, Zong Wenjun. Research on the Method of Reducing Dynamic Cutting Force in Aspheric Machining // Micromachines. 2023. Vol. 14. № 5. Article number 960. DOI: 10.3390/mi14050960.
26. Ellersiek L., Menze C., Sauer F., Denkena B., Möhring H.-Ch., Schulze V. Evaluation of methods for measuring tool-chip contact length in wet machining using different approaches (microtextured tool, in-situ visualization and restricted contact tool) // Production Engineering. 2022. Vol. 16. № 5. P. 635–646. DOI: 10.1007/s11740-022-01127-w.
27. Vukelic D., Simunovic K., Ivanov V., Sokac M., Kocovic V., Santosi V., Santosi Z., Simunovic G. Modelling of Flank and Crater Wear during Dry Turning of AISI 316L Stainless Steel as a Function of Tool Geometry Using the Response Surface Design // Tehnicki Vjesnik – Technical Gazette. 2024. Vol. 31. № 4. P. 1376–1384. DOI: 10.17559/tv-20231226001235.
28. Younas M., Khan M., Jaffery S.H.I., Khan Z., Khan N. Investigation of tool wear and energy consumption in machining Ti6Al4V alloy with uncoated tools // The In-

ternational Journal of Advanced Manufacturing Technology. 2024. Vol. 132. № 7-8. P. 3785–3799. DOI: 10.1007/s00170-024-13548-1.
29. Çiftçi I. Machining of austenitic stainless steels using CVD multi-layer coated cemented carbide tools // Tribology International. 2006. Vol. 39. № 6. P. 565–569. DOI: 10.1016/j.triboint.2005.05.005.
30. Gokkaya H., Taşkesen A. The effects of cutting speed and feed rate on BUE-BUL formation, cutting forces and surface roughness when machining AA6351 (T6) alloy // Journal of Mechanical Engineering. 2008. Vol. 54. № 7-8. P. 521–530.

Оценка влияния состава сплава на параметры обработки и качество поверхности посредством комплексного анализа

Шайлеш Рао Агари*[1], кандидат наук, профессор, факультет машиностроения
Рао Шрилата[2], кандидат наук, профессор
Технологический институт Нитт Минкши, Бангалор (Индия)

***E-mail:** shailesh.rao@nmit.ac.in

[1]ORCID: https://orcid.org/0000-0001-6190-9857
[2]ORCID: https://orcid.org/0000-0003-3691-8713

Поступила в редакцию 25.04.2024 *Пересмотрена 18.06.2024* *Принята к публикации 05.11.2024*

Аннотация: Изучалось влияние состава сплавов (мягкой стали и алюминия) на несколько параметров обработки, таких как температура, сила резания, шероховатость поверхности и морфология стружки. Значительные изменения этих параметров были обнаружены путем модификации сплавов при поддержании постоянных условий процесса. В мягкой стали скорость вращения влияла на морфологию стружки, при этом повышенные скорости приводили к образованию непрерывной стружки, а пониженные скорости – к образованию более короткой стружки. Увеличенный передний угол влияет на свойства стружки, что приводит к небольшому уменьшению ее длины. При заданной скорости вращения на длину стружки влияла сила резания. Алюминиевые сплавы, напротив, производили непрерывные фрагменты стружки независимо от скорости резания или переднего угла. Были выбраны коэффициенты корреляции переменных, разработана эффективная регрессионная модель и применена к экспериментальным данным. Модель случайного леса показывает, что выбор материала существенно влияет на температуру, силу резания, шероховатость поверхности и морфологию стружки во время обработки. Получены данные о корреляции между передним углом инструмента и другими параметрами обработки, выявлены факторы, влияющие на качество поверхности. Результаты способствуют лучшему пониманию свойств обработанной поверхности, что облегчает оптимизацию операций обработки для различных материалов.

Ключевые слова: токарная обработка; передний угол; морфология стружки; прогнозное моделирование.

Для цитирования: Шайлеш Рао А., Рао Ш. Оценка влияния состава сплава на параметры обработки и качество поверхности посредством комплексного анализа // Frontier Materials & Technologies. 2024. № 4. С. 97–110. DOI: 10.18323/2782-4039-2024-4-70-9.